



Research paper

Load-bearing capacity analyses of a new insulated fastener type

Tomasz Janiak¹

Abstract: Balconies are elements of some multi-storey buildings. Thermo-insulated fasteners are components that connect balcony slabs with the building structure. Their main task is the transfer of loads in connections of balcony slabs with the building while also minimizing thermal bridges. The article presents analytical calculations performed to develop the new type of thermal insulated fasteners and to determine their load-bearing capacity. The aim of this article is to demonstrate that analytical calculations based on commonly utilized principles of reinforced concrete and steel structure operation along enable the development of the effective design algorithm of insulated fasteners and allow for a quick analysis of various geometric variants of these fasteners. The article presents the adaptation of typical algorithms for calculation of steel and reinforced concrete structures for the analysis of non-typical load-bearing capacity states that occur during the calculation of insulated fasteners. The load-bearing capacities of individual fasteners are shown in $M-V$ interaction diagrams (bending moment – shearing force).

Keywords: thermal insulated fasteners, load capacity, calculation algorithm

¹PhD., Eng., Bydgoszcz University of Science and Technology, Faculty of Civil and Environmental Engineering and Architecture, Al. prof. S. Kaliskiego 7, 85-796 Bydgoszcz, Poland, e-mail: tomasz.janiak@pbs.edu.pl, ORCID: 0000-0001-9460-1963

1. Introduction

Balconies are elements of multi-storey residential buildings and some public buildings. They form a certain useful floor space that allows direct, wider contact with the environment and is usually used for short-term recreation. Not until quite recently, that is a dozen or so years ago, were the balconies installed directly to the building structure. Thermal insulation layers used on the external side of the walls resulted in braking of the insulation continuity and formation of thermal bridges. Modern standards and regulations related to building energy efficiency (i.e. Directive of the European Parliament and of the Council of the European Union [1]) largely limit the possibility of using those classic methods of balcony installations in new buildings. Such solutions are possible, but troublesome, because the balcony slab must be insulated in a continuous manner.

The issues of energy saving and the related thermal insulation of buildings are analyzed by many researchers (e.g. [2,3]). In order to minimize the effect of thermal bridges between balcony and building structures, a number of systemic thermal insulation solutions for balcony fasteners have been developed. The task of thermo-insulated balcony fasteners is to join the balcony structure (usually in the form of a reinforced concrete balcony slab) with the building structure while maintaining some empty space between them. There are supporting elements and thermal insulation in the empty space zone. Moreover, the space is limited at the bottom and at the top with elements which ensure the connection is fire-resistant.

From the structural point of view, balcony fasteners are designed to transfer bending moments and vertical shear forces from the balcony structure to the building structure. Apart from that, fasteners may be exposed to other loads, e.g. horizontal forces parallel to the fastener due to temperature difference between the balcony and building structure. As a rule, these interactions can be omitted by utilizing structural expansion joints with appropriate joint spacing. Load-bearing elements of balcony fasteners can be round steel bars capable of transmitting mainly axial forces, steel or high quality concrete inserts capable of transmitting possible compression and shear forces, and steel profiles transmitting shear forces and bending moments. These elements must be designed primarily for bearing capacity conditions. Fasteners, as building structural elements, must also provide sufficient durability. Sufficient corrosion protection of reinforcement bars in reinforced concrete structures is provided with a suitable, thick concrete surround. The steel elements in the area between the balcony and the building structure are only covered with thermal and fire insulation. It does not protect against corrosion and, moreover, makes it impossible to control the condition of these elements and to recreate anti-corrosion coatings. The solution is to use stainless steel grades, which are additionally feature approx. 3.4 times lower heat transfer coefficient compared to standard steel.

It is worth mentioning that attempts are being made to use materials other than steel and concrete in balcony fastener production. Analyses on the use of fiber-reinforced polymer (FRP) supported with studies were carried out. As reinforcement, glass fiber (GFRP), or aramid fiber (AFRP) can be used. Thermal conductivity of such composites is up to 170 times lower than that of stainless steel, which is their huge advantage [4–6]. Attempts to replace steel elements with GFRP fiber composites have not yet been made in industry [7–9].

Only a relatively few studies on thermal insulation of balcony fasteners have been created. The analyses of a new system solution for balcony fasteners were presented by Keo at al. [10, 11]. An improved fastener system was considered there, made of reinforcement bars with additional elements, subject to forces in different directions. Fastener fatigue strength was also taken into account.

Functional and structural elements similar to balcony fasteners were analyzed in the study [12]. The studies related to the thermal-insulating fasteners between external walls and the load-bearing support slab in buildings with thermal insulation on the inner side of walls (in such cases the classic connection of floor slabs with walls creates linear thermal bridges). Attempts were made to reproduce loads on these elements during an earthquake. Advanced numerical analyses and laboratory tests of fasteners were carried out there.

Another, much less frequently used solution for the balcony construction is the utilization of a reinforced concrete slab based on steel cantilever beams, which are fixed to the building structure. In this case, point thermal bridges are formed. Examples of thermal and mechanical analyses of such balconies are presented in studies [13–15].

Apart from thermal insulation and mechanical strength of fasteners, other aspects of their application were also studied. For example, vibration transmission through fastener supporting elements was analyzed in [16, 17].

A new type of thermo-insulating balcony fasteners was analyzed in this study. The main load-bearing elements of these fasteners are two parallel Ω -shaped rods (hat channels) made of stainless steel. Hat channels are connected to properly shaped reinforcing bars, the task of which is to transmit stresses between hat channels and the balcony and building structure. They study discusses the geometry and structural assumptions related to fasteners.

The main objective of the these activities was to develop an effective structure of balcony fasteners as well as calculation algorithms for quick analysis of load capacity of various geometrical variants of these fasteners. The developed calculation algorithm for fast, analytical calculations of fastener capacity is presented. Basic assumption for its development was to use the principles of reinforced concrete and steel structure analysis contained in the Eurocodes. It proved necessary to adapt these principles in the non-typical calculation models that were identified in the fastener analysis.

2. Fastener description

A single balcony fastener consists of two Ω -shaped channels (hat section) and four U-shaped reinforcement bars welded with them. The basic fastener type with dimensions is shown in Fig. 1a. Central parts of hat channels of the connection are located in the area that is not set in concrete, between the balcony slab concrete and the building structure. One of the fastener ends is cast in the balcony slab and the other one – in the building structure. The hat channel with cross-section geometry shown in Fig. 1b, is made of stainless steel. This ensures that central fastener parts that are not in cast will not corrode. The second benefit is lower heat transfer coefficient of stainless steel compared to standard steel. The drawing shows main central axes of this profile. As it can be seen, the profile center of

gravity is at half of its height. U-shaped reinforcement bars are welded to hat channels. These bars connect the top profile to the bottom profile and, at the same time, ensure the transfer of forces between the fastener and concrete of the building and balcony structure.

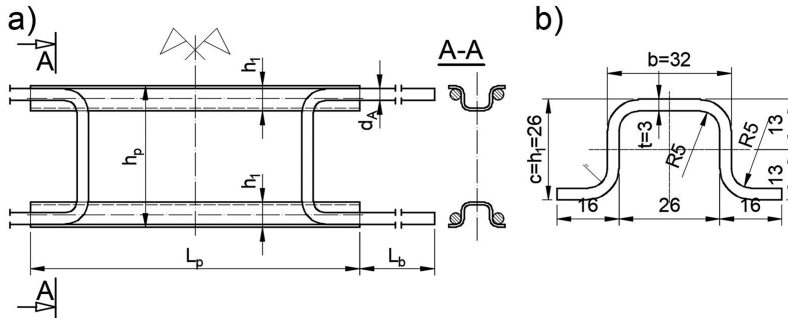


Fig. 1. Balcony fastener – standard type: a) fastener view and section view; b) hat channel geometry

Fig. 2 shows the connection between the balcony slab and the floor structure with a balcony fastener. The fastener must be selected according to the thickness of load-bearing plates H and connection width L in order to ensure the required minimum surround values a_b , a_{b2} , and a_p .

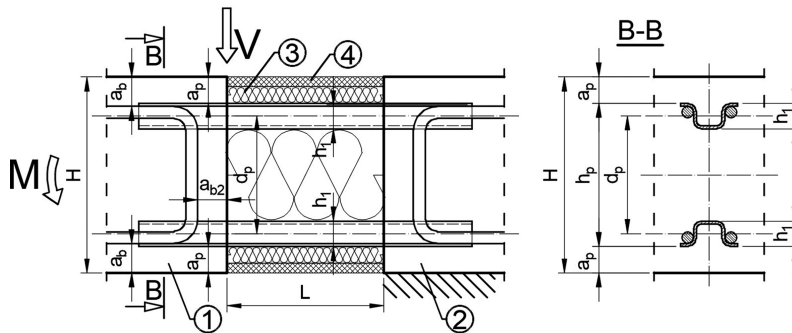


Fig. 2. Connection between the balcony slab to the floor slab with a balcony fastener; 1 – balcony slab; 2 – floor slab; 3 – thermal insulation; 4 – fire insulation

3. Analysis of fastener behavior

Fastener analysis can be divided into two stages. During the first stage, based on the steel structure design, hat channels in the space between the balcony slab and the building structure will be considered. In the second stage, based primarily on the theory of reinforced concrete structures, the fastener anchorage zones in the concrete of the balcony and building structure will be analyzed.

A shear force V and a bending moment M act on a single fastener (see Fig. 2). The values of these forces result from the structural static analysis of the balcony slab performed by the designer. Remaining internal forces, including torsional moments and normal forces, are considered negligible. The stiffness of concrete blocks of a balcony and a ceiling into which the fastener is inserted are so large in comparison with bending stiffness of the hat channels that the reinforced concrete elements are considered as rigid, non-deformable bodies. Static diagram for the analysis of hat channels in the zone without concrete (space width L) is presented in Fig. 3. It was assumed that the Ω profiles work in the linear elastic range, and that the compressed profile (lower in Fig. 3) may buckle. It was also established that the basic geometric dimensions of the connectors, i.e. the plate thickness H (see Fig. 2) and the width L , will be limited to the values resulting from the practice of using the connectors in construction. Finally, the connectors meeting the following conditions were analyzed: $16 \text{ cm} \leq H \leq 24 \text{ cm}$, $L \leq 20 \text{ cm}$.

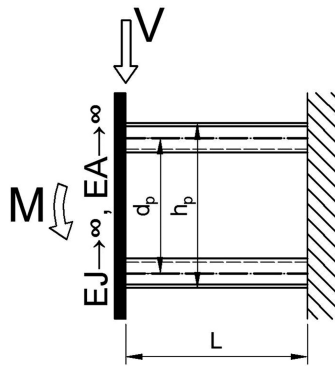


Fig. 3. Static diagram for hat channels in thermal insulation zone between balcony and floor slabs

The purpose of analyses was to determine a set of such force pairs (M , V) that would not lead to exceeding the hat channel capacity. It is assumed that the channels will operate in a linear elastic state. This assumption means that no permanent plastic deformation will occur in the element material.

When analyzing the static diagram shown in Fig. 3, the influence of force V and moment M was analyzed separately. Taking into account the force V for hat channels, the diagrams of shear forces T_V and bending moments M_V shown in Fig. 4 are obtained.

Shear forces cause shear stress. These stresses (their maximum value in cross-section) were determined on Eq. (3.1) based on Eq. (6.20) of standard [18].

$$(3.1) \quad \tau_{Ed} = \frac{T_V S_1}{2I_1 t}$$

where: $T_V = \frac{1}{2}V$ – value of shearing force acting on a single hat channel (see Fig. 4), S_1 – static moment of a part of the hat channel section located above the center of gravity (see Fig. 1b), I_1 – channel moment of inertia, t – wall thickness.

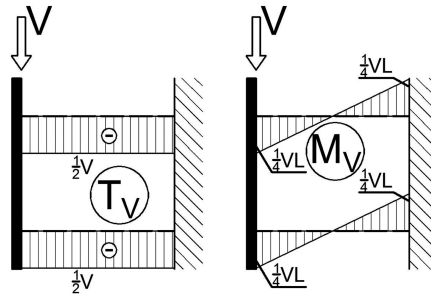


Fig. 4. Graphs of V force-induced cutting forces and bending moments

Taking into account Eq. (6.19) of standard [18], the first load condition that limits the V force is formulated. It is the following:

$$(3.2) \quad \frac{\tau_{Ed}}{f_y^p} = \frac{VS_1}{(4I_1t f_y^p)} \leq 1$$

$$\frac{(\sqrt{3}\gamma_{M0})}{(\sqrt{3}\gamma_{M0})}$$

where: f_y^p – yield strength of hat channel material, γ_{M0} – partial factor in accordance with [19].

Bending moments create normal stresses in hat channel bar cross-sections. The graph of these stresses in $\alpha - \alpha$ section is shown in Fig. 5.

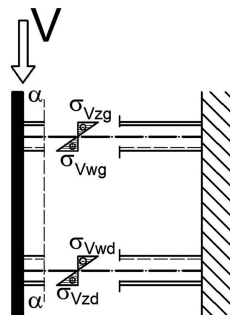


Fig. 5. Graph of normal stresses in $\alpha - \alpha$ section induced with V force

Taking into account the fact that the center of gravity of the hat channel is half of its height, all stresses shown in Fig. 5 are equal in absolute value (i.e. $|\sigma_{Vzg}| = |\sigma_{Vwg}| = |\sigma_{Vwd}| = |\sigma_{Vzd}|$) and can be marked with the symbol σ_V . These stresses are defined with the Eq. (3.3)

$$(3.3) \quad \sigma_V = \frac{M_{V,\alpha}}{W_1}$$

where: $M_{V,\alpha}$ – value of bending moment in the section $\alpha - \alpha$ of a single hat channel, $W_1 = 2I_1/c$ – bending section modulus of a hat channel.

The highest σ_V stress values are found at the edges of balcony and floor slabs, and their value is the following:

$$(3.4) \quad \sigma_{V,ekstr} = \frac{VL}{4W_1}$$

In case of the analysis of M moment-induced stress, the fastener is assumed to behave as a built-up cross-section (an alternative, simplified approach is to replace the moment with a pair of forces and assume that the upper hat channel stretched and the lower hat channel is compressed). There are the same normal stresses in each vertical section — their diagram is shown in Fig. 6.

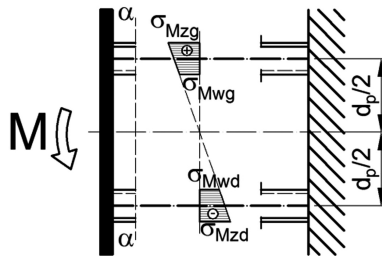


Fig. 6. Graph of normal stress induced with moment M

In this case, the stresses σ_{Mzg} and σ_{Mzd} are extreme and equal in absolute value. These values are indicated with a common symbol σ_M . They are defined with the following relationship:

$$(3.5) \quad \sigma_M = \frac{M}{W}$$

where: W – bending section modulus for a built-up cross-section.

With force V and moment M acting at the same time, normal stresses shown in Fig. 5 and 6 are added. Their maximum value must meet the material strength condition, from which hat channels are made. This results in a second condition related to (M, V) load pairs acting on a single fastener:

$$(3.6) \quad \sigma_{ekstr} = \sigma_{V,ekstr} + \sigma_M = \frac{VL}{4W_1} + \frac{M}{W} \leq \frac{f_y^p}{\gamma_{M0}}$$

When bending a built-up cross-section, one of its branches is mainly compressed. Bending moment can be replaced with a pair of forces with an arm equal to d_p – the axial spacing of hat channels (see Fig. 3 and 6). Compression force of the lower branch will have a value determined with Eq. (3.7).

$$(3.7) \quad N = \frac{M}{d_p}$$

A simplified analysis of the compressed branch stability was performed in accordance with point 6.3 of the standard [16] and point 5.4 of the standard [17] (in particular Eq. (6.49)–(6.51) from the standard [16] and Eq. (5.6)–(5.9) of the standard [17] were used). The parameters of imperfection $\alpha = 0.49$, maximum slenderness ratio $\lambda'_0 = 0.4$, and buckling length $L_{cr} = L$ were assumed.

The fastener anchorage zones in balcony and floor concrete slabs must also be capable of carrying the load pair (M, V) . The verification of anchorage zone capacity related to moment M is performed in a relatively simple manner. It has already been mentioned, the bending moment M acting on the fastener can be replaced with a force pair. These forces will be transmitted to the reinforced concrete elements through reinforcement bars of diameter d_A (see Fig. 1a), welded to hat channels. It was assumed that the moment M must be transmitted only with a force pair that act in the reinforcement bar axes. Based on the connection geometry shown in Fig. 2, another condition can be formulated to limit the range of permissible values M . The condition is the following Eq. (3.8).

$$(3.8) \quad \frac{M}{(H - 2a_b - d_A)} \leq 2 \frac{f_y^p}{\gamma_s} \frac{\pi d^2}{4}$$

The left side of the Eq. (3.8) expresses the value of a force pair that balance the moment M . The right side is the calculated capacity value of two reinforcement bars of diameter d_A . Reinforcing steel yield strength is indicated with f_y^p and γ_s is the partial material factor specified in point 2.4.2.4 of the standard [20].

In case of force V the problem of load-bearing capacity of the anchorage zone of the fastener in the concrete is more complex. The first state under consideration is related to the capacity of the upper hat channel against pulling it out of concrete. The procedure used here is based on the method of simplified dimensioning of single-bent reinforced concrete sections based on the standard [20]. The geometry of the analyzed anchorage zone and the forces and stresses within this zone are presented in Fig. 7.

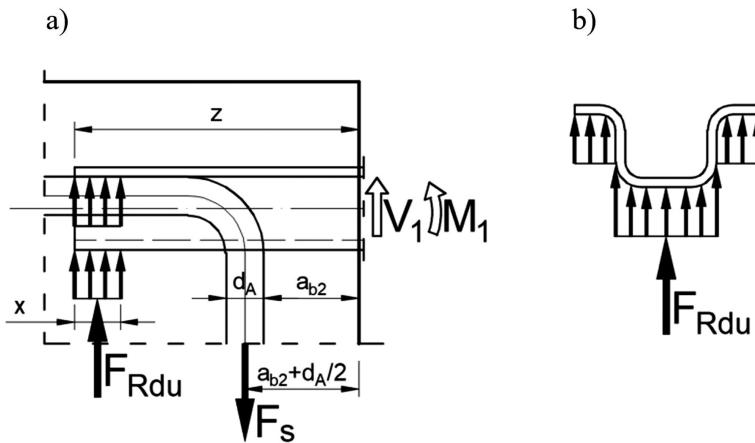


Fig. 7. Distribution of forces and stresses acting on the hat channel in the fastener anchorage zone in the balcony slab

The forces V_1 and M_1 shown in Fig. 7a are, respectively, shear force and the V force-induced bending moment operating in a hat channel bar section that is flush with the edge of the balcony slab. The internal force diagrams shown in Fig. 4 show that $V_1 = \frac{1}{2}V$, and $M_1 = \frac{1}{4}VL$. F_{Rdu} is the resultant of stresses in concrete. This resultant is determined as the bearing capacity (Eq. (6.63) of the standard [20]), when acting on a surface with a length x and width of the entire hat channel (see Fig. 7b). It means that F_{Rdu} is a function of variable length x . F_s is the force in both reinforcement bars welded to the hat channel. The determination of forces F_{Rdu} and F_s comes down to solving two equations:

$$(3.9) \quad 0.8F_{Rdu} \left(z - \frac{x}{2} - \frac{d_A}{2} - a_{b2} \right) - V_1 \left(\frac{d_A}{2} + a_{b2} \right) - M_1 = 0$$

$$(3.10) \quad F_{Rdu} - F_s + V_1 = 0$$

Eq. (3.9) denotes the sum of moments relative to any point in the line of action of the force F_s . The solution of this equation allows to determine the force F_{Rdu} and range of the stress zone x . An additional condition was introduced to limit this zone range:

$$(3.11) \quad \frac{x}{\left(z - \frac{d}{2} - a_{b2} \right)} \leq 0.4$$

After determining the force F_{Rdu} based on Eq. (3.10), which is a condition for force equilibrium in a vertical direction, the force F_s can be calculated. This force may not exceed the tensile strength capacity of two reinforcement bars:

$$(3.12) \quad F_s \leq 2 \frac{f_y^p}{\gamma_s} \frac{\pi d^2}{4}$$

The procedure described above, based on the use of Eq. (3.9), (3.10), and additional conditions (3.11) and (3.12), introduces further limitation of the maximum force value V . In order to verify the assumptions and the above described dependencies limiting the bearing capacity of the upper hat channel against pulling it out of concrete, it was decided to perform verification laboratory tests (not presented in this paper).

Another limitation, or rather a recommendation, to be taken into account when determining the maximum force V , is related to shear strength and punching shear strength of a reinforced concrete balcony slab. This verification is the responsibility of structural designers who select the fasteners. With large fastener spacing, their influence on the plate is basically in a point. It was therefore recommended that, when checking only the shear condition, the width of the plate band carrying the shear stress should be limited in the calculation. It was recommended that the width of such a band should not be greater than twice the useful height of the reinforced concrete section (the height in the standard [20] is marked with the d symbol). This means that the width of the reinforced concrete band carrying

shear force from one fastener must not exceed the value b_w determined by Eq. (3.13).

$$(3.13) \quad b_w = 2 \left(H - a_b - \frac{d}{2} \right)$$

The markings used in the Eq. (3.13) are shown in Fig. 1 and 2. Obviously, the width b_w cannot be larger than fastener spacing.

Finally, the area of permissible (M, V) force values is limited as shown in Fig. 8.

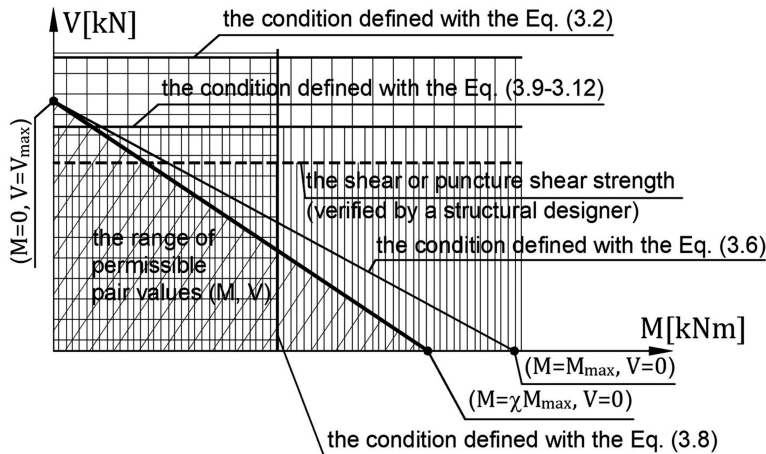


Fig. 8. Graph of permissible (M, V) force pair values related to all load conditions

During the calculation it turned out that the shear strength of hat channels, as determined by Eq. (3.2), was in each case greater than the V_{\max} value, and therefore did not in fact limit the range of permissible (M, V) pair values. Fastener shear strength is also limited by the condition set out in the Eq. (3.9)–(3.12). It is easily visible that the length of the hat channel insert in the concrete is essential in terms of this limitation (z dimension showed in Fig. 7). Finally, the z dimension was chosen so that the shear force limitation based on Eq. (3.9)–(3.12) is also greater than the V_{\max} value. This was to make full use of the hat channel load capacity.

4. Results

The developed calculation algorithm was used to calculate the load capacity of the size range of balcony fasteners to be introduced into production. Most of the data necessary for the calculation was obtained from the future fastener manufacturer.

The following material data of balcony fastener elements were adopted:

- Reinforcement bar steel: with a characteristic yield strength f_{yk} or $f_{0.2k}$ of 500 MPa; $\gamma_s = 1.15$; reinforcement bar diameter $d = 12$ mm;
- Hat channel steel: stainless steel with yield strength of $f_y \geq 640$ MPa, $\gamma_{M0} = 1.1$;

The calculations assume that concrete strength class of the building and balcony slab structure will not be lower than C20/25. Material parameters of the concrete were adopted according to [20].

The following geometrical data were adopted (designations according to Fig. 2):

- H [cm] = {16, 18, 20, 22, 24}; L [cm] = {12, 16}; $a_b = a_{b2} = 3.0$ cm; $a_p = 2.7$ cm;
- Cross-sectional geometry of hat channels – according to Fig. 1b;
- $z = 9.0$ cm – hat channel insert in concrete (see Fig. 7).

Taking into account the data summarized above, load capacity conditions discussed earlier have been checked. As a result, the M - V interaction graphs showing the ranges of permissible (M , V) force pairs acting on a single fastener were obtained. These graphs take into account the load bearing capacity of hat channels and reinforcement bars. An example of the final M - V interaction graph, concerning a fastener with a width of $L = 16$ cm, is shown in Fig. 9.

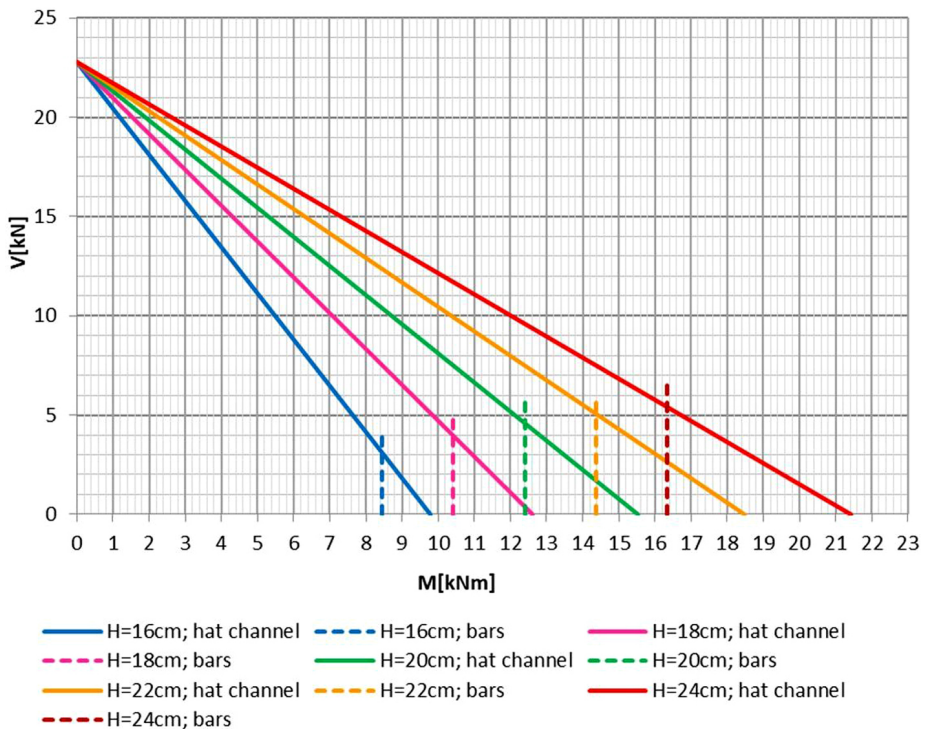


Fig. 9. M - V interaction graph for a single fastener with a width of $L = 16$ cm, with balcony panel thickness (16, 18, 20, 22, 24) [cm]

Analogous calculations, leading to the creation of a graph and strength tables, were prepared for fasteners of size $L = 12$ cm and $L = 8$ cm.

5. Summary and final conclusions

The subject of the analyses discussed in this study was the new type of insulated balcony fasteners. A new solution in their construction was the use of hat channels (hat-shaped) made of stainless steel. Such channels provide a good connection with floor and balcony slab concrete (better than tubular sections with concrete cavity, not filled inside). At the same time, they feature favorable geometrical characteristics (moments of inertia and bending section moduli) both for a single branch and for the entire built-up cross-section.

The paper presents an original, fast and relatively simple analytical calculation algorithm for determining the load-bearing capacity of fasteners. It was used to calculate the load-bearing capacity of a series of fastener types consisting of two fastener widths and five load-bearing plate thicknesses. Selected calculation results are presented in the paper.

From the very beginning, the main assumption of the conducted activities was to develop a solution for balcony fasteners that can be commercialized. Apart from tests discussed in the article, the fasteners in question passed the tests carried out in the Building Research Institute (Instytut Techniki Budowlanej, ITB). Their positive performance assessment was confirmed in the “National Technical Assessment” document issued by the Institute. On these grounds, the fastener production deployment and sales was started.

References

- [1] E.U. EU, Directive 2018/844/EU Energy performance of buildings, Off. J. Eur. Union, 2018.
- [2] P. Nowak, M. Skłodkowski, “Multicriteria analysis of selected building thermal insulation solutions”, *Archives of Civil Engineering*, 2016, vol. 62, no. 3, pp. 137–148, DOI: [10.1515/ace-2015-0088](https://doi.org/10.1515/ace-2015-0088).
- [3] A. Życzyńska, T. Cholewa, “The profitability analysis of enhancement of parameters of the thermal insulation of building partitions”, *Archives of Civil Engineering*, 2014, vol. 60, no. 3, pp. 335–347, DOI: [10.2478/ace-2014-0023](https://doi.org/10.2478/ace-2014-0023).
- [4] K. Goulouti, J. De Castro, A.P. Vassilopoulos, T. Keller, “Thermal performance evaluation of fiber-reinforced polymer thermal breaks for balcony connections”, *Energy and Buildings*, 2014, vol. 70, pp. 365–371, DOI: [10.1016/j.enbuild.2013.11.070](https://doi.org/10.1016/j.enbuild.2013.11.070).
- [5] K. Ghazi Wakili, H. Simmler, T. Frank, “Experimental and numerical thermal analysis of a balcony board with integrated glass fibre reinforced polymer GFRP elements”, *Energy and Buildings*, 2007, vol. 39, pp. 76–81, DOI: [10.1016/j.enbuild.2006.05.002](https://doi.org/10.1016/j.enbuild.2006.05.002).
- [6] K. Goulouti, J. de Castro, T. Keller, “Aramid/glass fiber-reinforced thermal break – Structural system performance”, *Composite Structures*, 2016, vol. 152, pp. 455–463, DOI: [10.1016/j.compstruct.2016.05.038](https://doi.org/10.1016/j.compstruct.2016.05.038).
- [7] T. Keller, F. Riebel, A. Zhou, “Multifunctional hybrid GFRP/steel joint for concrete slab structures”, *Journal of Composites for Construction*, 2006, vol. 10, no. 6, DOI: [10.1061/\(ASCE\)1090-0268\(2006\)10:6\(550\)](https://doi.org/10.1061/(ASCE)1090-0268(2006)10:6(550)).
- [8] T. Keller, F. Riebel, A. Zhou, “Multifunctional all-GFRP joint for concrete slab structures”, *Construction and Building Materials*, 2007, vol. 21, no. 6, DOI: [10.1016/j.conbuildmat.2006.06.003](https://doi.org/10.1016/j.conbuildmat.2006.06.003).
- [9] K. Goulouti, J. de Castro, T. Keller, “Aramid/glass fiber-reinforced thermal break – thermal and structural performance”, *Composites Structures*, 2016, vol. 136, pp. 113–123, DOI: [10.1016/j.compstruct.2015.10.001](https://doi.org/10.1016/j.compstruct.2015.10.001).
- [10] P. Keo, B. Le Gac, H. Somja, F. Palas, “Experimental study of the behavior of a steel-concrete hybrid thermal break system under vertical actions”, in *High Tech Concrete Where Technology Engineering Meet, Jun 2017, Maastricht – Proc. 2017 Fib Symposium*, 2017, pp. 2573–2580, DOI: [10.1007/978-3-319-59471-2_293](https://doi.org/10.1007/978-3-319-59471-2_293).
- [11] P. Keo, B. Le Gac, H. Somja, F. Palas, “Low-cycle fatigue life of a thermal break system under climatic actions”, *Engineering Structures*, 2018, vol. 168, pp. 525–543, DOI: [10.1016/j.engstruct.2018.04.063](https://doi.org/10.1016/j.engstruct.2018.04.063).

- [12] T.T.H. Nguyen, F. Ragueneau, D. Bahon, N. Ruaux, "Macroscopic modeling of reinforced concrete joints: Application to thermal break elements subject to earthquake loadings", *Engineering Structures*, 2014, vol. 79, pp. 131–141, DOI: [10.1016/j.engstruct.2014.08.001](https://doi.org/10.1016/j.engstruct.2014.08.001).
- [13] A. Ben Larbi, M. Couchaux, A. Bouchair, "Thermal and mechanical analysis of thermal break with end-plate for attached steel structures", *Engineering Structures*, 2017, vol. 131, pp. 362–379, DOI: [10.1016/j.engstruct.2016.10.049](https://doi.org/10.1016/j.engstruct.2016.10.049).
- [14] D.B. Cleary, W.T. Riddell, N. Camishion, P. Downey, S. Marko, G. Neville, M. Oostdyk, T. Panaro, "Steel Connections with Fiber-Reinforced Resin Thermal Barrier Filler Plates under Service Loading", *Journal of Structural Engineering*, 2016, vol. 142, no. 11, DOI: [10.1061/\(ASCE\)ST.1943-541X.0001576](https://doi.org/10.1061/(ASCE)ST.1943-541X.0001576).
- [15] L. Nasdala, B. Hohn, R. Rühl, "Design of end-plate connections with elastomeric intermediate layer", *Journal of Constructional Steel Research*, 2007, vol. 63, no. 4, DOI: [10.1016/j.jcsr.2006.06.022](https://doi.org/10.1016/j.jcsr.2006.06.022).
- [16] M. Schneider, H.M. Fischer, "Vibration reduction of thermal break balcony connections", *Journal of the Acoustical Society of America*, 2008, vol. 123, DOI: [10.1121/1.2935551](https://doi.org/10.1121/1.2935551).
- [17] S. Bailhache, M. Villot, C. Guigou-Carter, P. Jean, "Vibration reduction indexes of façade T junctions with thermal bridge break or composed of more than two building element types", presented at Forum Acusticum 2014, September 7–12, Krakow, Poland, 2014.
- [18] EN 1993-1-1, E. 1993-1-1 CEN, *Eurocode 3. Design of steel structures. General rules and rules for buildings*, Eurocode 3. 2005.
- [19] E. 1993-1-4, E. 1993-1-4 CEN, *Eurocode 3. Design of steel structures. Part 1-4: General Steels, Supplementary rules for stainless*, Eurocode 3. 2006.
- [20] EN-1992-1-1 *Eurocode 2 – Design of concrete structures Part 1-1: General rules for buildings, Part 1–1 Gen. Rules Rules Build.* 2008.

Analizy nośności termoizolacyjnych łączników balkonowych nowego typu

Słowa kluczowe: termoizolacyjne łączniki balkonowe, nośność, algorytm obliczeniowy

Streszczenie:

Termoizolacyjne łączniki balkonowe są elementami łączącymi płyty balkonowe z konstrukcją budynków. Ich zadaniem jest zminimalizowanie mostków termicznych w tych połączeniach. Zasadniczymi częściami składowymi takich łączników są elementy nośne, warstwa termoizolacyjna oraz warstwy izolacji zapewniające ogniotrwałość połączenia. Przedmiotem niniejszego artykułu są elementy nośne łączników.

Artykuł prezentuje obliczenia analityczne termicznych łączników balkonowych nowego typu, umożliwiające określenie nośności tych łączników. Omówiona została również konstrukcja i idea pracy statycznej tych łączników.

Opracowując artykuł postawiono sobie za cel wykazanie, że obliczenia analityczne oparte na powszechnie stosowanych zasadach pracy konstrukcji żelbetowych i stalowych (omówionych m.in. w Eurokodach) połączone z badaniami laboratoryjnymi wybranych przypadków (nie omówionych w niniejszym artykule) umożliwiają opracowanie skutecznej koncepcji konstrukcyjnej łączników balkonowych oraz pozwalają na szybką analizę różnych wariantów geometrycznych tych łączników.

Zasadniczymi elementami nośnymi rozważanego pojedynczego łącznika balkonowego są dwa równoległe, umieszczone jeden nad drugim pręty wykonane ze stali nierdzewnej. Elementy te są połączone za pomocą przyspawanych prętów zbrojeniowych. Pręty zbrojeniowe zapewniają dodatkowo odpowiednie połączenie łączników z płytą nośną balkonu i konstrukcją budynku. W artykule przedstawiono opartą na Eurokodach analizę podstawowych stanów granicznych takich łączników,

tj. stanu nośności na zginanie i stanu nośności na ścinanie. Analizie podlegały elementy stalowe oraz beton przejmujący naprężenia z tych elementów. Konieczna przy tym była odpowiednia adaptacja algorytmów normowych. Omówiono metodologię obliczeń nośności łączników oraz przedstawiono wybrane wyniki nośności dla różnych wariantów geometrycznych. Nośności pojedynczych łączników pokazano na wykresach interakcji $M-V$ (moment zginający – siła ścinająca).

Opracowane łączniki ostatecznie przeszły pozytywnie badania wykonane w Instytucie Techniki Budowlanej. Ich pozytywna ocena właściwości użytkowych została potwierdzona w wydanym przez ten Instytut dokumencie “Krajowa Ocena Techniczna”.

Received: 02.08.2021, Revised: 07.12.2021